

Anharmonicity of bridging oxygen oscillations in $\text{YBa}_2\text{Cu}_3\text{O}_{7-x}$ crystals

L. V. Gasparov, V. D. Kulakovskii, V. B. Timofeev, and V. Ya. Sherman

Institute of Solid State Physics, USSR Academy of Sciences; Moscow Physicotechnical Institute

(Submitted 18 July 1991)

Zh. Eksp. Teor. Fiz. **100**, 1681–1689 (November 1991)

Raman scattering (RS) of light is used to investigate the behavior of the oxygen modes in $\text{YBa}_2\text{Cu}_3\text{O}_{7-x}$ crystals with different oxygen contents ($0 < x < 1$) as a function of exciting-radiation power and of temperature. The excitation spectra of these modes are measured. Two-phonon RS is observed in $\text{YBa}_2\text{Cu}_3\text{O}_{6.5}$ crystals. To explain the behavior of the investigated modes it is proposed that the bridging-oxygen ion O4 is located in an anharmonic two-well potential.

INTRODUCTION

The spectra of Raman scattering (RS) of light by $\text{YBa}_2\text{Cu}_3\text{O}_{7-x}$ contain, besides the lines whose existence follows directly from a symmetry analysis of the phonon modes at the Γ point, additional lines, for example one near 590 cm^{-1} , which manifests itself most intensely in zz polarization. The appearance of this line is differently treated in various papers. In Refs. 1–3, for example, it is attributed to the IR-active mode that appears in RS spectra as a result of the lifting of the alternate hindrance in the presence of defects in positions of both chain and bridging oxygen. In Ref. 4 it is attributed to unit-cell doubling with respect to parameter a , produced in $\text{YBa}_2\text{Cu}_3\text{O}_{6.5}$ crystals by vacancy ordering in the chains, while in Refs. 5 and 6 it is attributed to interaction of photoexcited carriers with the lattice.

We shall show in the present paper, on the basis of the entire aggregate of the experimental results, that in crystals with disturbed oxygen stoichiometry ($0 < x < 1$) the ≈ 500 and $\approx 590 \text{ cm}^{-1}$ modes are closely connected and are due to oscillations of bridging O4 oxygen in a two-well potential.

1. EXPERIMENTAL TECHNIQUE AND SAMPLES

The experiments were performed with a Microdil-28 spectrometer having a microscope attachment that made it possible to monitor a location on the sample accurate to $10 \mu\text{m}$. An Ar^+ laser was used for the excitation. All experiments except those on the resonant dependence on the exciting-radiation wavelength were carried out with the $\lambda = 487.9865 \text{ nm}$ laser line. The resonance dependence of the RS intensity was investigated using a discrete set of Ar^+ laser lines.

A helium cryostat was used for the low-temperature measurements. The sample was mounted on a cold finger cooled by flowing liquid helium. The sample temperature was maintained at 20 K.

The high-temperature measurements were made with a Linkham TH 600 heat bath with a temperature regulator that made possible experiments up to temperatures of order 600°C accurate to 1°C . A microscope attachment was used in all the experiments.

The experiments were performed on $\text{YBa}_2\text{Cu}_3\text{O}_{7-x}$ single crystals with different oxygen contents ($x \approx 0.1; 0.5; 0.8$). Crystals with $x \approx 0.5$ were obtained by cooling from the melt without further finishing. The superconducting temperature of these crystals was $T_c = 60 \text{ K}$ and the transition width was about 10 K. Crystals with $x \approx 0.1$ were obtained by low-temperature annealing of samples with $x \approx 0.5$ in an

oxygen stream. These crystals had a superconducting temperature $T_c = 90 \text{ K}$ with an approximate transition width about 5 K. Crystals with $x \approx 0.8$ were made by annealing sample with $x \approx 0.5$ in an argon atmosphere. They did not become superconducting. All the crystals were rectangular slabs measuring $2 \times 2 \times 0.2 \text{ mm}^3$ with a specular basal plane. The experiments were made on fresh cleaved surfaces. The oxygen concentration was estimated from the frequency of the RS line corresponding to Ag oscillations of ions of bridge oxygen O4. This line predominates in zz -polarization spectra (Fig. 1), and its frequencies are $\approx 500, \approx 488, \text{ and } \approx 475 \text{ cm}^{-1}$ at $x \approx 0.1, 0.5, \text{ and } 0.8$, respectively.⁷

2. EXPERIMENTAL RESULTS

2.1. Experiments with variation of pump power

The first group of experiments of this kind was performed with samples at 20 K, and the second at room temperature. The exciting-radiation pump power was correspondingly changed and the intensity ratio of the ≈ 500 and $\approx 590 \text{ cm}^{-1}$ was investigated.

The results of these experiments are shown in Figs. 2–5. It can be seen that when the pump is increased the intensity ratio of the ≈ 590 and $\approx 500 \text{ cm}^{-1}$ lines increases noticeably. The excited-region temperature at maximum pump power (1200 mW laser output, corresponding to ≈ 400

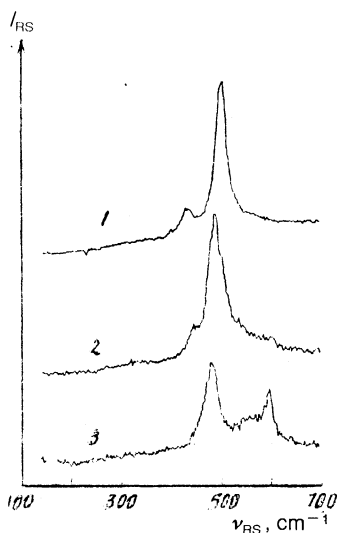


FIG. 1. Spectra of RS of light in $\text{YBa}_2\text{Cu}_3\text{O}_{7-x}$ crystals with different \bar{x} at low pump powers ($P = 50 \text{ mW}$) and at temperature $T = 300 \text{ K}$: 1— $x = 0.1$; 2— $x = 0.5$; 3— $x = 0.8$. Polarization ($x(zz)\bar{x}$).

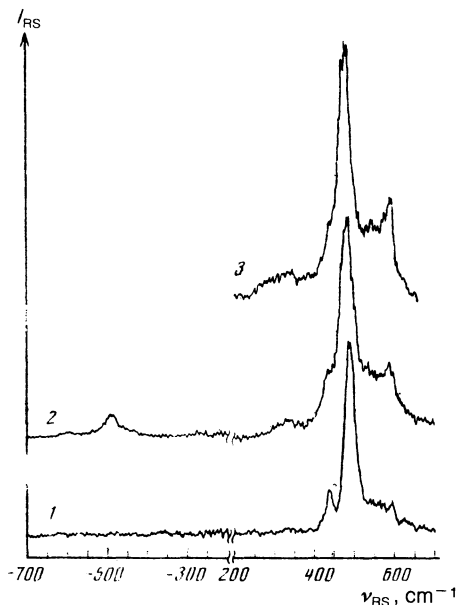


FIG. 2. Spectra of RS of light in $\text{YBa}_2\text{Cu}_3\text{O}_{6.5}$ crystal at $T = 20$ K (1,2) and $T = 300$ K (3), at pump powers $P = 150$ mW (1,3) and 1200 mW (2). Polarization $(x(zz)\bar{x})$.

W/mm^2 on the sample) in the first group of experiments (in the cryostat at $T = 20$ K) the excited-region temperature estimated from the intensity ratio of the Stokes and anti-Stokes spectrum components, did not exceed 300°C .

In the experiments of the second group the peak intensity of the investigated lines was normalized to the peak intensity of the 220 cm^{-1} line in a BaF_2 crystal. As seen from Fig. 3, as the pump power to the $\text{YBa}_2\text{Cu}_3\text{O}_{6.5}$ crystal is increased the normalized intensity of the $\approx 500\text{ cm}^{-1}$ line decreases, and that of the $\approx 590\text{ cm}^{-1}$ line increases. The corresponding increase and decrease of the intensities of these modes is reversible, just as in the first group of experiments. As to the $\approx 330\text{ cm}^{-1}$ line corresponding to antiphase oscillations of the oxygen ions O2 and O3 in the $\text{Cu}_2\text{-O}_2\text{-O}_3$

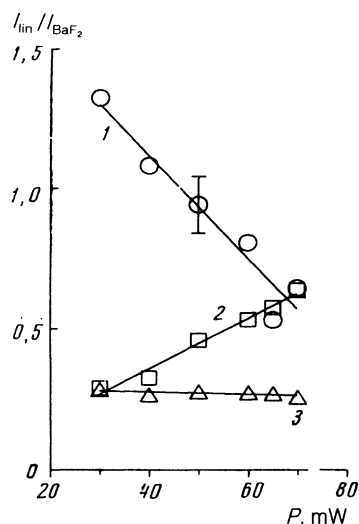


FIG. 3. Dependence of normalized intensities of the lines $\approx 500\text{ cm}^{-1}$ (curve 1), $\approx 590\text{ cm}^{-1}$ (curve 2), and $\approx 330\text{ cm}^{-1}$ (curve 3) on the pump power. Polarization $(x(zz)\bar{x})$ for the ≈ 500 and $\approx 590\text{ cm}^{-1}$ modes and $(x(\gamma\gamma)\bar{x})$ for the $\approx 330\text{ cm}^{-1}$ mode. Crystal $\text{YBa}_2\text{Cu}_3\text{O}_{6.5}$, $T = 300$ K.

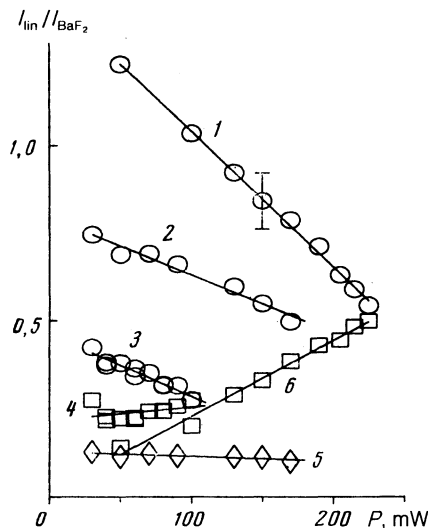


FIG. 4. Dependence of normalized line intensities on the pump power. Curves 1 and 6—for $\text{YBa}_2\text{Cu}_3\text{O}_{6.5}$ crystal, 2 and 5—for $\text{YBa}_2\text{Cu}_3\text{O}_{6.9}$, and 3 and 4—for $\text{YBa}_2\text{Cu}_3\text{O}_{6.2}$. For the $\approx 500\text{ cm}^{-1}$ mode (curves 1, 2, and 3), $\approx 590\text{ cm}^{-1}$ (curves 4 and 6) and $\approx 430\text{ cm}^{-1}$ (curve 5). Polarization $(x(zz)\bar{x})$, $T = 300$ K.

plane (curve 3 of Fig. 3), its intensity remains unchanged. Figure 4 shows for crystals with different oxygen contents the dependences of the intensities of the line corresponding to oscillations of the bridge oxygen O4 ($\approx 500\text{ cm}^{-1}$, curves 1-3), of the $\approx 590\text{ cm}^{-1}$ line (curves 4 and 6), and of the line corresponding to the in-phase oscillations of the oxygen O2 and O3 in the $\text{Cu}_2\text{-O}_2\text{-O}_3$ plane ($\approx 430\text{ cm}^{-1}$, curve 5). It can be seen that power at which the intensities of the ≈ 500 and $\approx 590\text{ cm}^{-1}$ become equalized is different for different crystals.

When the pump power is increased, the intensity of the 500 cm^{-1} line in $\text{YBa}_2\text{Cu}_3\text{O}_{6.9}$ crystals decreases, while the $\approx 590\text{ cm}^{-1}$ line does not appear all the way to the maximum pump power that does not destroy the sample surface ($\approx 500\text{ mW}$). Depending on the pump, the rate of decrease of the $\approx 500\text{ cm}^{-1}$ line intensity is approximately half that

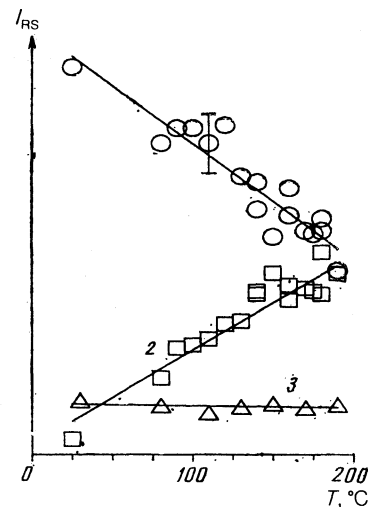


FIG. 5. Temperature dependences of the intensities of the lines ≈ 500 , ≈ 590 , and $\approx 330\text{ cm}^{-1}$ (curves 1, 2, and 3). The polarization is $(x(zz)\bar{x})$ for the ≈ 500 and $\approx 590\text{ cm}^{-1}$ modes and $(x(\gamma\gamma)\bar{x})$ for $\approx 330\text{ cm}^{-1}$. $\text{YBa}_2\text{Cu}_3\text{O}_{6.5}$ crystal.

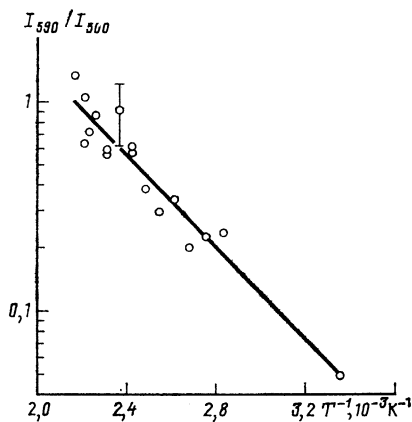


FIG. 6. Logarithm of the intensity ratio of the 590 and 500 cm^{-1} lines in $(x(zz)\bar{x})$ polarization spectra vs the reciprocal temperature. $\text{YBa}_2\text{Cu}_3\text{O}_{6.5}$ crystal.

in crystals with 6.5 oxygen content. The normalized intensity of the $\approx 430 \text{ cm}^{-1}$ line remains in this case practically constant (curve 5 of Fig. 4).

In crystals with oxygen content 6.2 the situation is similar to that with oxygen content 6.5, except that in the zz spectrum of these crystals the lines ≈ 590 and $\approx 500 \text{ cm}^{-1}$ are close in intensity even at low pump powers (see Fig. 1). With increase of pump power, the normalized intensity of the $\approx 590 \text{ cm}^{-1}$ line increases, but substantially more slowly (by ≈ 6 times) than in $\text{YBa}_2\text{Cu}_3\text{O}_{6.5}$ crystals.

2.2. High-temperature experiments

As seen from Fig. 5, when $\text{YBa}_2\text{Cu}_3\text{O}_{6.5}$ crystals are heated the peak intensity of the $\approx 500 \text{ cm}^{-1}$ line decreases, that of the $\approx 590 \text{ cm}^{-1}$ increases, and that of the $\approx 330 \text{ cm}^{-1}$ line remains unchanged. The ratio of the line intensities in the temperature interval from 300 to 500 K can be approximated by the exponential relation (Fig. 6):

$$I_{590}/I_{500} \approx A \exp(\Delta/T) \quad (1)$$

with $\Delta \approx 2500 \pm 30 \text{ K}$, $A \approx 230 \pm 20$.

Since the temperature interval of our experiments was substantially smaller than Δ , the value obtained must be refined, as it will in future experiments.

Close to 200°C the intensities of the ≈ 500 and $\approx 590 \text{ cm}^{-1}$ modes become equalized, i.e., as the temperature is raised the lines behave in the same way as when the pump power is lowered, and all the changes take place with bridging and possibly chain oxygen, but not with planar O2 and O3 oxygen ions (the intensity of the $\approx 330 \text{ cm}^{-1}$ line corresponding to counterphase oscillations of these ions does not change).

Note that the increase of the intensity of the $\approx 590 \text{ cm}^{-1}$ mode cannot be reduced to an increase of the Bose factor since, as seen with the $\approx 500 \text{ cm}^{-1}$ mode as the example, the variation of the line intensity with temperature is not described by this law.

When the temperature is raised the frequencies of both modes decrease. In the 300–500 K interval the “softenings” amounted to 13 and 7 cm^{-1} for the ≈ 500 and $\approx 590 \text{ cm}^{-1}$ modes, respectively.

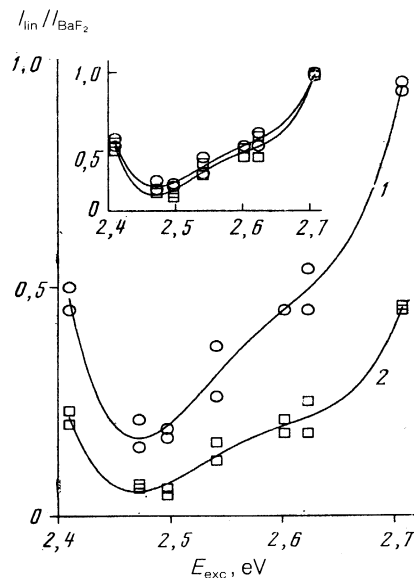


FIG. 7. Normalized intensities of ≈ 500 (1) and $\approx 590 \text{ cm}^{-1}$ (2) lines vs the exciting-radiation frequency. Polarization $(x(zz)\bar{x})$, temperature 410 K, crystal $\text{YBa}_2\text{Cu}_3\text{O}_{6.5}$.

2.3. Resonance and polarization dependences

The dependences of the intensities of the ≈ 500 and $\approx 590 \text{ cm}^{-1}$ lines, normalized to the intensity of the BaF_2 line, on the exciting-radiation energy are shown in Fig. 7. The inset shows the same dependences, but each normalized to the maximum value. These dependences are evidently identical. This indicates that the character of the scattering is governed by the electronic properties of the complex Cu1-O4-O1 (Refs. 8 and 9) (i.e., identical hybridized electronic states participate in the scattering). This conclusion is confirmed also by experiments on the polarization properties of scattering by the $\approx 590 \text{ cm}^{-1}$ mode. For this mode, just as for $\approx 500 \text{ cm}^{-1}$, one observes a substantial predominance of the scattering intensity in zz polarization over scattering in xx and yy polarizations, noted also in Ref. 10.

3. DISCUSSION

To estimate the intensities of single-phonon Raman scattering by the investigated modes, we use an adiabatic approximation in which the scattering tensor corresponding to a generalized coordinate Q is of the form

$$P_{\alpha\alpha}(\omega, Q) = Q \partial P_{\alpha\alpha} / \partial Q, \quad (2)$$

where

$$P_{\alpha\alpha} = \sum | \langle i | \mathcal{M}_\alpha | m \rangle |^2 \frac{2\omega_{mi}}{\omega_{mi}^2 - \omega^2} \quad (2a)$$

is the polarizability tensor. Here m and i denote the initial and final electronic states over which the summation is carried out, d is a Cartesian coordinate, and \mathcal{M}_α is a component of the dipole-moment vector. The scattering intensities $I_{\alpha\alpha}$ are proportional to the square of the matrix elements $P_{\alpha\alpha}$ on the phonon wave functions. The states i and m are taken to be p_z orbitals of the O4 oxygen ions and the $d_{y^2-x^2}$ orbitals of the Cu1 ions.⁸ Since the overlap of the orbitals is in this case of σ type, the dependences of the matrix elements in (2a) on the displacement of the O4 ion should be very strong.

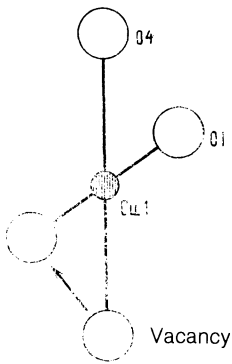


FIG. 8. Configuration of O1, O4, and Cu1 ions at which Raman-active oscillation of the O4 ion with frequency $\approx 590 \text{ cm}^{-1}$ sets in.

To explain the experimental data we must assume the following:

a) The potential energy of the O4 oxygen ion should have two minima as a function of the coordinate. The presence of an O4 oxygen ion at one of the minima is manifested in RS as the $\approx 500 \text{ cm}^{-1}$ mode, and at the other as the $\approx 590 \text{ cm}^{-1}$ mode;

b) transitions of an oxygen ion between these minima are initiated by temperature, and the process should be reversible.

Such potential-energy minima can be, for example, the positions of the O4 oxygen and vacancies produced at the location of the O1 oxygen in the case of an oxygen deficit. When the crystal is heated the O4 ion can leave its place and land on one of the free places in the plane of the ions Cu1 and O1. Then, owing to breaking of one of the Cu1–O4 bonds, the remaining O4 oxygen ion (Fig. 8) has an oscillation frequency close to that of the IR-active mode constituting mainly in-phase oscillations of a pair of O4 oxygen ions with frequency $\approx 600 \text{ cm}^{-1}$ (Ref. 11). Owing to the strong symmetry breaking, this oscillation of the O4 ion becomes allowed in Raman scattering. At the same time, the fully symmetric oscillation corresponding to the $\approx 500 \text{ cm}^{-1}$ mode vanishes in this process. The departure of O4 ions (observed in experiment already at $T \approx 450^\circ \text{C}$ (Ref. 12) accounts for the decrease of the intensity of the $\approx 500 \text{ cm}^{-1}$ mode, and the substantial change of the electronic structure of the bond explains the matrix-element increase that contributes to the increase of the scattering intensity. The presence of a $\approx 590 \text{ cm}^{-1}$ mode in $\text{YBa}_2\text{Cu}_3\text{O}_{6.2}$ crystals may be due here to the presence of defects in the positions of the O4 ions which appear at a large oxygen deficit.

On the other hand, the second minimum can be some position close to the O4 ion and not connected with the displacement of the O4 oxygen in the Cu1–O1 plane. The hopping distances will be shorter than in the first case, i.e., we assume that the experimental data reported above can be attributed to the presence, in the scattering Cu1–O4–O1 complex, of a two-well potential for the O4 ion (Fig. 9) under conditions of violation of the oxygen stoichiometry. At low temperatures, the oxygen ion is localized mainly in potential well 1 and oscillation with $\omega \approx 500 \text{ cm}^{-1}$ appears in the system. When the temperature is raised, the particle can land by tunneling or activation in well 2 located closer to the Cu1 ion, and this leads to the appearance of the $\approx 590 \text{ cm}^{-1}$ mode.

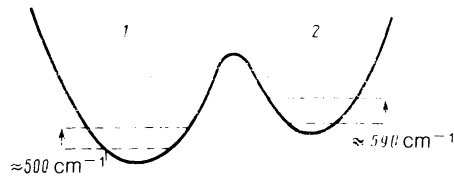


FIG. 9. Two-well potential for bridging O4 oxygen.

The proximity of the potential well 2 to the Cu1 ion increases the components of the scattering tensor by decreasing the Cu1–O4 bond length, i.e., increasing the matrix elements contained in (1) and of their derivatives, and also on account of the stronger dependences of these components of the tensor \mathcal{P}_{aa} on the coordinate Q . The result is an increase of the scattering intensity per ion, so that the intensities of scattering by the ≈ 500 and $\approx 590 \text{ cm}^{-1}$ can become equalized even at low particle density in the potential well 2.

An important question in this model is the ratio of the time to establish thermodynamic equilibrium system to the time of the experiment. To this end, we examine qualitatively the factors influencing the establishment of equilibrium.

We take the energy-measurement unit to be the energy-level spacing $\hbar\omega$ in well 1, and the unit of length measurement to be the “amplitude” of the zero-point oscillations $x_0 = (\hbar/M\omega)^{1/2}$ (M is the oxygen-ion mass and is the oscillation frequency corresponding to well 1), and write for the dependence of the ion energy on the displacement:

$$U(x) = \frac{1}{2}x^2 + \sum \beta_n x^n, \quad (3)$$

β_n are anharmonic parameters that depend on the type of crystal and on the oxygen content. Estimates in terms of the lattice parameters show that $\beta_n \sim (m/M)^{(n-2)/4}$ (m is the electron mass). Since $(m/M)^{1/4} \sim 0.1$, all the terms in the sum (3) are of the same order at $x \sim 10x_0$, and consequently the characteristic distance between potential wells is $\sim 10x_0$. If we confine ourselves in the estimate of the tunneling probability to cubic anharmonicity, a quasiclassical estimate of the time to establish equilibrium via the tunneling mechanism yields

$$\tau_t \sim \omega^{-1} \exp(1/15\beta_3^2). \quad (4a)$$

Under the same assumptions, the “activation” time for onset of equilibrium is

$$\tau_a \sim \omega^{-1} \exp(W/T), \quad (4b)$$

W is the height of the potential barrier and equals $\hbar\omega/54\beta_3^2$. Thus, in a temperature region $\sim \hbar\omega$ these probabilities become equalized, and it is possible that the principal role is played in our experiments not by the tunneling but by the activation mechanism.

Note that in this model there is a direct connection between the probability of tunneling from region 1 into region 2 and the second-harmonic intensity for the $\approx 500 \text{ cm}^{-1}$ mode, since both phenomena are due to anharmonicity of the initial potential. Simple calculations yield (assuming that the entire contribution to the second-harmonic intensity comes from the anharmonicity of the potential)

$$\tau_t \sim \omega^{-1} \exp(I_2/15I_1), \quad (4c)$$

I_1 and I_2 are the intensities of the corresponding harmonics

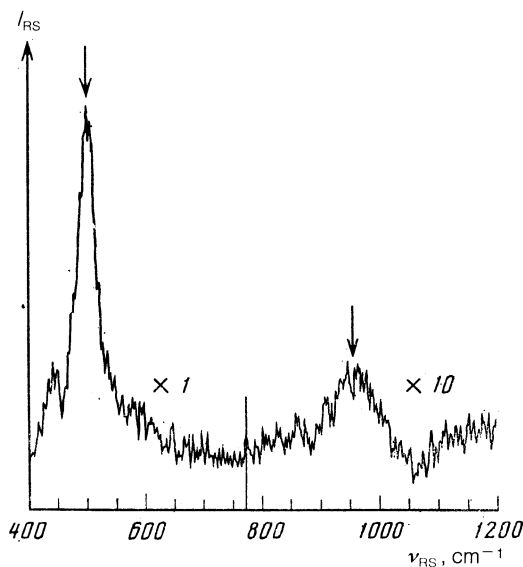


FIG. 10. RS spectrum in $\text{YBa}_2\text{Cu}_3\text{O}_{6.5}$ crystal from 200 to 1100 cm^{-1} at low pump intensities. The arrows mark the first and second harmonics of the mode connected with the O4 oxygen oscillations at $\approx 490 \text{ cm}^{-1}$ and $\approx 960 \text{ cm}^{-1}$, respectively. Polarization ($x(z?)\bar{x}$).

at low pump intensities.

If the characteristic distance between wells is of the order of ten zero-point-oscillation amplitudes, it is necessary to take into account in the dependence of the potential energy on the coordinate a large number of “nonlinear” terms, but the estimates obtained above remain in force. Note that in this case an important role can be played by the numerical factors that determine the probability of tunneling or of activation umklapp, and also the dependence of the tunneling time on particle energy (on the number of the state from which this tunneling is effected).

Under conditions of strong anharmonicity it is natural to expect two-photon scattering processes to be manifested in the RS spectra. We have succeeded in observing second-order Raman scattering in the $\text{YBa}_2\text{Cu}_3\text{O}_{6.5}$ crystal (Fig. 10). The ratio of the peak intensities of the two-phonon and single-phonon scatterings was approximately 0.03. It is possible, however, that this quantity is due not to the anharmonicity of the potential itself, but to a strong electron-photon interaction that allows a second harmonic to appear even in the absence of anharmonicity.

Note that since the dependence of the tunneling on the potential parameters (ω and β_n) that can vary with the oxygen content in the investigated sample is exponential, even small changes of the anharmonicity and of the natural frequency can change substantially the tunneling time. In crystals with small oxygen deficit and high superconducting temperature the anharmonicity is small, and the frequency ω is a maximum, so that no $\approx 590 \text{ cm}^{-1}$ modes are observed in the RS spectrum.

The values of ω and β_n can vary not only from sample to sample, but can also be different for different configurations of one and the same crystal with a non-stoichiometric oxygen composition. Thus, for example, in crystals with oxygen content close to 6.5 there can apparently be realized a configuration in which the minimum of the second potential

well lies somewhat lower than that of the first, and contains an oxygen ion even at $T = 0$. This corresponds to observation of a “defective” mode at low pump powers. With increase of the oxygen deficit, the number of such configurations increases, but the anharmonicity decreases. This increases the intensity of the $\approx 590 \text{ cm}^{-1}$ mode at low pump powers and to weak increase of this intensity as a function of the pump intensity.

When samples with low oxygen density ($x \approx 0.8$) are prepared, there can also be produced metastable states corresponding to localization of the O4 ion in well 2. When crystals with $x \approx 0.5$ are heated, some of the ions land in well 2, with increase of the oxygen density in the Cu1–O1 chains and with increase of the order in the system, the anharmonicity also decreases. The probability of reverse tunneling when the sample is cooled becomes thus small, and these ions can turn out to be “frozen” in well 2.

The temperature dependence of the frequencies of the investigated modes, noted by us in Sec. 2.2, indicates that various changes of the potential can occur in the course of heating. This can lead to a redistribution of the ions among the potential wells. This question requires further investigation.

CONCLUSION

We have investigated the nonlinear properties of Raman scattering of light in $\text{YBa}_2\text{Cu}_3\text{O}_{7-x}$ crystals with different x . We regarded the properties of modes of frequency ≈ 500 and $\approx 590 \text{ cm}^{-1}$ as manifestations of nonlinearity. The experimental data can be interpreted on the basis of notions concerning different types of two-well potentials produced in the Cu1–O1–O4 complex. For a more complete study, new experiments are necessary, such as on the dependence of the scattering intensity at various temperatures on the applied external pressure. It is possible that this will make possible a final choice favoring one treatment or another.

We take pleasure in thanking G. A. Emel’chenko and A. V. Krashennnikov for preparing the samples, A. A. Polyanskiĭ for supplying the cryostat, and T. V. Mukhin for help with the reduction of the experimental data. We are also indebted to O. V. Misochko for helpful discussions during the initial stage of the work.

¹ D. M. Krol, M. Stavola, W. Weber *et al.*, *Phys. Rev. B* **36**, 8325 (1987).

² R. Liu, C. Thomsen, W. Kress *et al.*, *ibid.* **37**, 7971 (1988).

³ K. F. McCarty, J. C. Hamilton, R. N. Shelton *et al.*, *ibid.* **38**, 2914 (1988).

⁴ G. Blumberg, E. M. Fefer, T. A. Frimberg *et al.*, *Pis'ma Zh. Eksp. Teor. Fiz.* **49**, 384 (1989) [*JETP Lett.* **49**, 439 (1989)].

⁵ V. N. Denisov, B. N. Mavrin, V. B. Podobedov *et al.*, *Phys. Lett. A* **130**, 411 (1988).

⁶ I. Poberaj, D. Mihailovic, and S. Bernik, *Phys. Rev. B* **42**, 393 (1990).

⁷ R. M. Macfarlane, H. J. Rosen, E. M. Engler *et al.*, *ibid.* **38**, 284 (1988).

⁸ E. I. Rashba and E. Ya. Sherman, *Pis'ma Zh. Eksp. Teor. Fiz.* **47**, 404 (1988) [*JETP Lett.* **47**, 482 (1988)].

⁹ L. V. Gasparov, G. A. Emel’chenko, V. D. Kulakovskii *et al.*, *J. Opt. Soc. Am. B* **6**, 440 (1989).

¹⁰ D. Mihailovic and C. M. Foster, *Sol. St. Comm.* **74**, 753 (1990).

¹¹ A. V. Bazhenov, *Fiz. Tverd. Tela (St. Petersburg)* **32**, 1517 (1990) [*Sov. Phys. Solid State* **32**, 885 (1990)].

¹² J. D. Jorgensen, H. Shaked, D. G. Hinks *et al.*, *Physica (Utrecht) C*, **153–155**, 478 (1988).

Translated by J. G. Adashko